Review | Vol. 8, No. 12 | 1 Dec 2018 | OPTICAL MATERIALS EXPRESS 3864
Optical Materials EXPRESS

Spatial solitons to mold random lasers in nematic liquid crystals [Invited]

SREEKANTH PERUMBILAVIL,[1] ARMANDO PICCARDI,[2] OLEKSANDR BUCHNEV,[3] GIUSEPPE STRANGI,[4,5] MARTTI KAURANEN,[1] AND GAETANO ASSANTO[1,2,6,*]

[1]*Laboratory of Photonics, Tampere University of Technology, FI-33101 Tampere, Finland*
[2]*NooEL - Nonlinear Optics and OptoElectronics Lab, University "Roma Tre", IT-00146 Rome, Italy*
[3]*Optoelectronics Research Centre, University of Southampton, SO17 1BJ Southampton, UK*
[4]*Department of Physics, Case Western Reserve University, Cleveland, OH 44106-7079, USA*
[5]*CNR-NANOTEC and Dept. of Physics, University of Calabria, IT-87036, Italy*
[6]*CNR-ISC, Inst. Complex Systems, IT-00185 Rome, Italy*
**assanto@uniroma3.it*

Abstract: Dye-doped nematic liquid crystals support random lasing under optical pumping, as well as reorientational optical spatial solitons acting as all-optical waveguides. By synergistically combining these two responses in a collinear pump-soliton geometry, the resulting soliton-enhanced random laser exhibits higher conversion efficiency and better directional properties. After a short account on random lasers and solitons in nematic liquid crystals – nematicons – we describe our experimental results on nematicon-molded random lasers.

1. Introduction

The last decades have witnessed substantial experimental and theoretical progress on random lasing in disordered systems, i. e., cavityless lasing via recurrent scattering [1]. The idea that a highly coherent process – such as laser action – can originate in disordered and diffusive systems has triggered several discussions about the fundamental mechanisms and the coherence of lasers. Nowadays, an overall consensus of possible random-lasing mechanisms has come forward and new challenges and opportunities in the area have been identified. At the same time, spatial optical solitons in nematic liquid crystals –nematicons- have reached a mature level of physical and technical understanding [2]. Hereby, after recalling the main features of reorientational nematicons and summarizing the state-of-the-art in the emerging field of random lasers, we describe how to mold and control the flow of random laser light by employing spatial solitons at a nonresonant wavelength in stimuli responsive complex fluids such as dye-doped nematic liquid crystals. We report our recent findings on demonstrating directional features and modulability of efficient random lasers which exhibit good beam quality and can be angularly steered via externally applied fields.

2. Reorientational spatial solitons in nematic liquid crystals: nematicons

Nematic liquid crystals (NLC) are uniaxial dielectric soft-matter in a fluid state, with their organic molecules exhibiting anisotropic polarizability, larger along their main axes than orthogonally. Therefore, their linear optical properties depend on the polarization of light and are easily affected by external stimuli perturbing the molecular distribution [3]. NLC can be prepared in planar cells with given boundary conditions, in order to ensure that the molecules are arranged in an ordered fashion, i. e., with average orientation along a direction named molecular director **n** despite positional randomness. When the order-parameter is close to unity, standard NLC respond as positive uniaxial crystals, with refractive indices $n_{//}$ and $n_{\perp}$ for electric fields parallel and orthogonal to the optic axis **n**, respectively, and

#347772 https://doi.org/10.1364/OME.8.003864
Journal © 2018 Received 8 Oct 2018; revised 12 Nov 2018; accepted 13 Nov 2018; published 21 Nov 2018

Optical Materials EXPRESS

$\Delta n = n_{//} - n_{\perp} \geq 0.2$. When extraordinarily-polarized light waves propagate in such dielectric, electric dipoles are induced in the elongated molecules and tend to react (through an orientation-dependent torque) to the electric field **E**, increasing both the orientation angle θ with respect to the wave-vector $\boldsymbol{k}$ and the corresponding refractive index $n_e = \frac{n_{//} n_{\perp}}{\sqrt{n_{\perp}^2 \sin^2\theta + n_{//}^2 \cos^2\theta}}$. Such light-induced angular reorientation minimizes the system energy and balances the elastic intermolecular forces in the liquid and the restoring forces from the boundaries. Since $n_{\perp} \leq n_e \leq n_{//}$ in positive uniaxials, the change of n_e versus θ provides a self-focusing Kerr-like response [4], which is saturable and nonlocal as it extends beyond the disturbance size [5].

If a finite light beam, in the extraordinary polarization, propagates in NLC, light induced reorientation yields a graded-index transverse profile which can confine the beam itself into a non-diffracting optical spatial soliton, so called nematicon [6,7]. Nematicons are stable nonlinear 2D + 1 wavepackets thanks to the NLC nonlocal and saturable responses [4]; they oscillate in amplitude and width as they propagate, and are walking solitons with Poynting vector $\boldsymbol{S}$ angularly displaced by the walk-off angle $\delta(\theta) = \arctan\left[\frac{(n_{//}^2 - n_{\perp}^2)\sin(2\theta)}{n_{//}^2 + n_{\perp}^2 + (n_{//}^2 - n_{\perp}^2)\cos(2\theta)}\right]$ with respect to the wave-vector $\boldsymbol{k}$ [8]. Nematicon waveguides can guide other co-polarized signals [9–11], can be routed/steered in the presence of external voltages or beams [12–18], other solitons [19,20], refractive index or birefringence perturbations [21–23], *etc* [2,6,7,24,25]. In the highly nonlinear regime nematicons can self-route [26–28], enhance spontaneous symmetry breaking [29] and exhibit beam bistability [30,31]. In guest-host material systems, such as dye-doped NLC, reorientational nematicons can coexist with other nonlinearities and nonlinear effects, including frequency tripling [32], spatio-temporal localization [33], thermo-optic response [34–36]. Hereby we address and describe another remarkable example of synergy between nonlinear responses.

3. Random lasing

Since firstly proposed by Letokhov in 1968 [37], random lasers have been intensely studied - both theoretically and experimentally - in a plethora of disordered systems (nanopowders, ceramics, liquid crystals, polymers and biological tissues, among others). Letokhov predicted that the combination of recurrent scattering and light amplification would lead to a new form of laser, spurring the creativity of scientists all over the world. The arbitrary walk of light waves inside random media, in fact, results in the confinement and localization of light within the material over distances long enough for optical amplification to overcome losses. While wave propagation in disordered media and light localization were described by P. Anderson with reference to vanishing propagation of electrons due to interference effects under very strong multiple scattering in disordered electronic lattices [38], this concept served as a model for metal-insulator transitions and has been widely adopted in optics to account for wave propagation in random media. In particular, when diffusive photon transport in completely disordered systems satisfies the condition $k\ell_t \leq 1$ (where k is the magnitude of the local wave-vector and ℓ_t is the transport mean free path of photons), almost complete localization of light waves occurs, termed strong localization. In this limit, light is brought to a stand still and engenders an inherent and cavity-free feedback mechanism. Conversely, weak optical localization is considered to be a particular case of interference, predicted and observed in random media and in partially ordered systems when $k\ell_t > 1$ (Mott-Ioffe-Regel criterion [39,40]). Because of the bosonic nature of the light quanta, the possibility of coherent

Optical Materials EXPRESS

amplification or coherent absorption (attenuation) of light arises, as these are absent in the electronic (fermionic) case. Indeed, coherent amplification is a non-conservative scattering process where the temporal phase coherence of a wave is preserved despite gain. Active random media have repeatedly proven to be suitable candidates for diffusive laser action, mainly because the resonant feedback in conjunction with multiple scattering eliminates the need for an external cavity as in regular lasers. Light localization and interference effects, which survive multiple scattering, have been invoked to explain the random laser action observed in quite a few exotic and complex active systems [41–48].

Initial experimental investigations on the Letokhov prediction reported strong amplification at the transition frequency of the gain medium, albeit no discrete line narrowing was observed [41,42,49]. Later measurements, performed by tightly focusing the pump beam on smaller disordered systems, allowed observing discrete and narrow-band lasing lines [43,44,50–53]. In these experiments, typical gain saturation was observed by analyzing the photon statistics, whereas the emission distribution was found to be random in time and in space. In the search for a mechanism that could explain the origin of these discrete laser peaks [54], various scenarios have been proposed. An early picture suggested that feedback arises from multiple random scattering events leading to the spontaneous formation of closed optical paths within the disordered medium [54,55]. As an alternative to this early picture, loop resonators with large refractive index contrast were proposed and it was found that finite size scatterers could substantially increase the refractive index in these resonators because of disorder correlation [56,57]. Lately, single shot experiments in weakly scattering systems provided another interesting point of view: in fact, the appearance of random spikes suggested that spontaneously emitted photons accumulate gain along extended paths [58,59]. These "providential photons" -generated at a given point in space- were thought to acquire enough gain by returning to the point where they were originated, activating a new lasing mode at each pump shot. Using time resolved spectroscopy, aiming to evaluate the decay rates of the modes, anomalous diffusion was found and confirmed the existence of long-lived modes [60]. More recently, Fallert *et al* also reported experimental evidence of coexisting extended and localized modes in diffusive systems characterized by $L/\ell_t >> 1$, being L the size of the specimen [61]. Although extended and long lived modes appear to be responsible for random laser action, they can only be obtained in specific configurations and cannot explain the experimental observations in their entirety. The next natural step in order to evaluate the role of extended and localized modes was to study their structure and distribution in disordered systems without gain; when gain is then introduced, the modes with the longest lifetime and lasing threshold become discrete and intense laser lines [62].

Nonetheless, the most debated arguments about random lasing remain the role of interference effects, whether the distinction between diffusive and random lasers is needed and whether coherent feedback is required to produce random lasing. The distinction between diffusive and coherent random lasers is hampered by the fact that multiple scattering can be regarded as an elastic process, thus interference effects are inherent to it. A simplified diffusive model enters the problem when interference effects are averaged out during long excitation pulses compared to the characteristic time of the scattering dynamics. However, narrow-band spectra in random laser materials need be modeled accounting for interference effects. On a different note, coherent feedback is not required for random lasing as optical cavities are not essential for obtaining coherent random laser emission. The characteristic 'Poissonian' photon statistics that characterizes the coherent emission of a laser source is observed when light is first-order (field) and second-order (intensity) coherent. Any mechanism that selects a specific narrow banded mode (for example a band-pass filter) gives rise to first-order coherence, whereas second-order coherence is obtained by gain saturation. A random laser can exhibit coherent emission irrespective of the localization of the modes and the amount of 'coherent' feedback because of the amplification of spontaneously emitted photons by stimulated emission. When the gain is large, the intensity will grow until the gain

Optical Materials EXPRESS

medium is saturated. In general, this tends to suppress the intensity fluctuations and give rise to second-order coherence. To these extents, after the first studies on micro and nano-powders dissolved in gain media [43,44], a plethora of other experiments followed on ceramic random laser [63], biological tissues and bovine semen [47,64], nano-imprinted DNA [65], conjugated polymers [66], semiconductor polycrystalline films [67], disordered photonic crystals [68], perovskites [69], and thermotropic liquid crystals [70–75], among many others. Liquid crystals, in particular, are stimuli responsive complex fluids, turbid in appearance, characterized by a scattering cross section up to six orders of magnitude larger than conventional isotropic fluids [76]. The external stimuli responsiveness of this class of materials makes them very promising for controlling the flow of random laser light. The spontaneous fluctuations of the molecular director in nematic liquid crystals lead to fluctuations in the local dielectric tensor, which is the main responsible for the (recurrent multiple) scattering in these systems, which can also be doped with active molecules to provide amplification.

The main challenges for the development of random lasing applications are: i) the electrical excitation; ii) the directional control of a collimated beam, since the light is usually emitted in an unpredictable way and over a broad range of angles. Meeting the first challenge would allow applications in display and lighting technology, the main issue being the electrical conductance of the used materials because of their intrinsic disorder and often-porous character; Williams *et al* performed initial studies of rare-earth-doped oxide powders that can be excited electrically [77]. The directional control is crucial for a wide range of random laser applications, from imaging to security scanning. Various solutions have been tried over the years, including fibers [78–81], microchannels [82], tailored pump [83], and nanostructures [84].

4. Random lasing with collinear near-infrared soliton and visible pump

In order to face the limitations about directionality and transverse profile of random laser emission in liquid crystals, we resorted to a configuration encompassing both a reorientational nonlinear response and random laser action under optical pumping; such combination, in which reorientation supports spatial solitons, could provide suitable solutions to the lack of beam-like features by the presence of an optical spatial soliton. At variance with the configuration demonstrated in Ref. [85] with orthogonal wave-vectors for pump and nematicon beams, we used a collinear geometry: a pulsed pump laser at wavelength within the absorption region of the guest-host and a continuous-wave (cw) near-infrared (NIR) source were both injected with wave-vectors along the z-axis of a 100μm thick glass cell containing the soft matter.

In such planar configuration, illustrated in Fig. 1, light propagated in the bulk of a thick sample of dye-doped NLC with optic axis **n** pre-oriented by mechanical rubbing at π/4 with respect to the input wave-vectors $\boldsymbol{k}_g \,/\!/\, \boldsymbol{k}_{NIR} \,/\!/\, \boldsymbol{z}$ in the principal plane *yz* [86]. The guest-host was the commercial E7 (Merck) doped with 0.3 wt % Pyrromethene 597 dye (Exciton), with refractive indices $n_{\parallel} = 1.71$ and $n_{\perp} = 1.52$ for electric field parallel and perpendicular to **n**, respectively.

Optical Materials EXPRESS

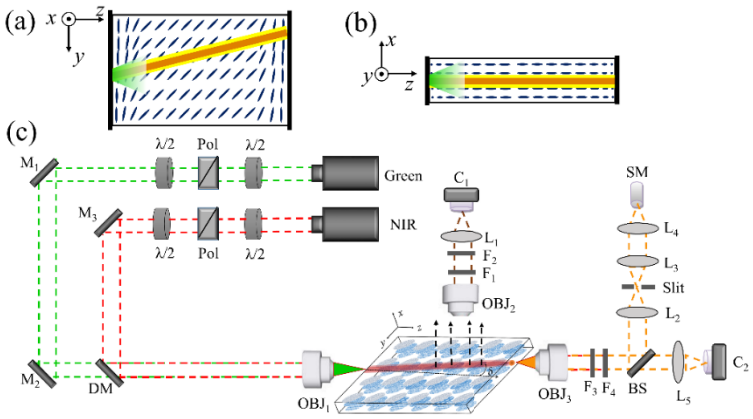

Fig. 1. (a) Top-view geometry of the planar NLC sample and experimental arrangement, with ordinary-wave green pump laser and extraordinary-wave NIR soliton injected with wave-vectors along z and propagating with the extraordinary-wave emitted light in the *yz* principal plane. (b) Side-view of the 2 mm-long 100 μm-thick sample, showing the emitted light confined within the nematicon. (c) Experimental set-up with pump (Green) and NIR sources and various optical elements: mirrors (M), dichroic mirror (DM), beam-splitter (BS), polarizers (Pol), half-wave plates (λ/2), filters (F), microscope objectives (OBJ), focusing lenses (L), cameras (C), spectrometer (SM). The angle δ identifies the birefringent walk-off with respect to the input wave-vectors and the dashed arrows represent out-of-plane scattering from the NLC.

A pump train of 6 ns pulses at 20 Hz and wavelength 532 nm was injected as an ordinary-wave (electric field oscillating along *x*) collinearly with an extraordinary-wave (electric field oscillating in *yz)* cw NIR beam (1064 nm), both gently focused to a radius of 3 μm at the entrance of the cell. The nonresonant NIR beam was able to form a nematicon at mW powers, the green pump provided gain by absorption and re-emission in the guest-host. Owing to anisotropic molecular scattering, pump-generated fluorescence, amplified spontaneous emission (ASE) and random laser (RL) emission were extraordinary-waves in this frustrated geometry [86,87] and could be confined within the cw-induced spatial soliton channel waveguide, propagating as guided-waves along the 2 mm long cell. Moreover, the energy flow (Poynting vector) of nematicon and guided emission evolved in the observation plane *yz* at the walk-off angle δ associated with extraordinary-waves in the positive uniaxial (see Fig. 1).

Fluorescence, laser emission and nematicon could be imaged versus propagation by means of out-of-plane scattered photons at the various wavelengths, as well as at the cell exit where undesired color components could be filtered out (see Fig. 1(c)). Figure 2 shows typical examples of an input NIR beam propagating in *yz* with $\boldsymbol{k}_{NIR} \,//\, \boldsymbol{z}$ as an ordinary-wave (Fig. 2(a)), a low-power extraordinary-wave (Fig. 2(b)) and a self-confined 5 mW nematicon (Fig. 2(c)); the birefringent walk-off $\delta = 7°$ is apparent.

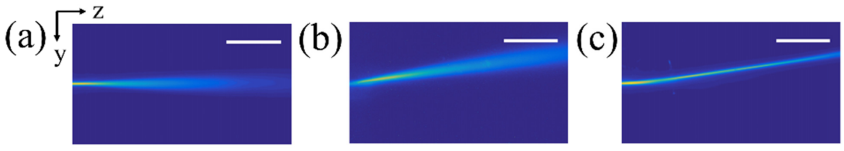

Fig. 2. Photographs (top-view) of (a) an ordinary-wave NIR beam diffracting in the observation plane *yz*; (b) an extraordinary-wave beam diffracting at low-power (0.7 mW) and propagating with walk-off; (c) a 5 mW extraordinary-wave beam self-confined into a nematicon and propagating with walk-off. The wavelength is 1.064 μm and the scale bars correspond to 500 μm.

Optical Materials EXPRESS

When pumping with pulses of sufficient energy to produce optical gain and overcome the system losses, the system turned into a random laser, oscillating in the wavelength range 570-590 nm with conversion efficiency and threshold clearly depending on the NIR soliton power. The solitary beam generated a graded-index waveguide which improved the collection efficiency of the emitted RL light and also enhanced the light-matter interaction between the pump and the emitted photons within the guided-wave region. Using a fiber-equipped spectrometer (resolution 0.15 nm) we analyzed the emitted light at the cell output acquiring spectra of single-realizations (individual pump laser pulses) versus energy/pulse and NIR power. Figure 3(a) shows a few examples of single-shot RL spectra when pumping at energies of 0.55 μJ and in the absence of NIR soliton. Figure 3(b) plots the corresponding average spectra $\bar{I}(\lambda)=\frac{1}{200}\sum_{k=1}^{200} I_k(\lambda)$ ($I_k(\lambda)$ are the individual emission intensity spectra), with a regular spacing of 0.7 nm between the RL spikes. In the absence of an external resonator, such periodicity suggests the presence of an equivalent cavity nearly 130μm long, related to the pump absorption length in the medium [88]. Finally, Fig. 3(c) displays the average output peak intensity $\bar{I}_{\max}=\frac{1}{200}\sum_{k=1}^{200}\max_{\lambda} I_k(\lambda)$ versus pump energy/pulse around the center emission wavelength (582 nm). It is clear that, above an energy threshold dependent on the input NIR power, the input-output characteristics show lasing with slope efficiencies which are significantly enhanced by the presence of the (pump-collinear) NIR soliton. Such efficiency increases with NIR power, whereas the energy threshold decreases, pinpointing how the cw nematicon improves the overall operation of this random laser. From averaged data, the RL conversion efficiency for a 6 mW nematicon with a 0.6 μJ pump, corrected for Fresnel losses at the cell facets and at the optical elements (F_3, F_4, OBJ_3 in Fig. 1(c)) amounts to a conspicuous 2.62% despite the propagation losses over the 2 mm-long sample.

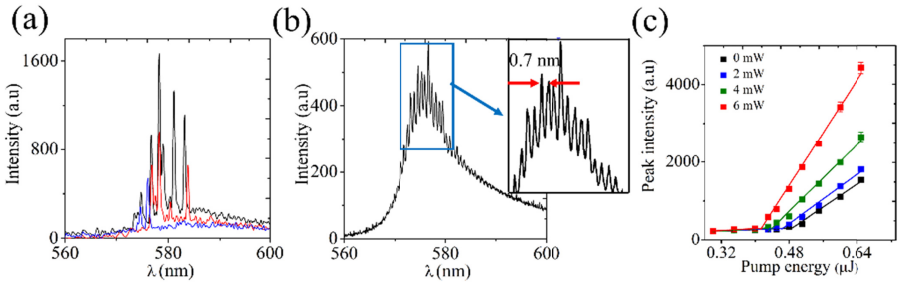

Fig. 3. (a) Three realizations of single-shot spectra (red, blue, black lines) of random laser emission when pumping at 0.55 μJ and without a collinear NIR nematicon. (b) Spectra averaged over N = 200 realizations when pumping at 0.55 μJ, with zoomed-in inset showing a regular wavelength spacing of 0.7 nm. (c) Input-output RL characteristics (average of peak intensities) for various powers of the collinear nematicon, as marked in the legend. The RL threshold shifts to lower energies as the input NIR power increases.

A synopsis of measured RL energy outputs and conversion efficiencies for various pump energies and soliton powers is provided in Table 1, after correcting for Fresnel and transmission losses as discussed above. Considering an "optimized" sample length corresponding to the size of the equivalent cavity (130 μm), i. e., minimizing scattering and absorption losses in the active guest-host, we can extrapolate the maximum obtainable output energies $(E_{out})_{max}$ and efficiencies η_{max}, as listed in the last two columns of Table 1. In this optimum limit for the examined geometry and mixture, a 6 mW nematicon assisted RL would convert 9.62% of the input 0.60 μJ pump energy into laser emission.

While such projected efficiency values could -in principle- be further increased by pumping at higher energies and/or injecting nematicons of higher NIR power, saturation and

Optical Materials EXPRESS

thermal effects, as well as bleaching, would have to be carefully accounted for. Saturating effects versus pump energies were observed and reported by us in earlier experiments and the same collinear configuration [90].

5. Transistor-laser operation

As noted above, when pumping the system with pulses above the lasing threshold, the presence of a collinear NIR-soliton modifies the output spectra through improved photon collection and interactions, as well as modified scattering. This is apparent not only in the characteristics graphed in Fig. 3(c), but also form single-pulse spectra collected at the output. Figure 4 displays several examples of individual RL spectral realizations versus near-infrared soliton power and for three values of input pump energy above threshold. It is clear that, at a given pumping level, a higher-power collinear soliton tends to enhance the random occurrence of sharp and intense lasing peaks over the background consisting of fluorescence and amplified spontaneous emission. Such trend can be interpreted in terms of better confinement of emitted light afforded by nematicon waveguides induced by higher NIR power.

Table 1. Measured RL energy output E_{out} and conversion efficiency η corrected for Fresnel losses and transmission of the optical elements for various pump energies/pulse E and NIR input beam powers P_{NIR}. Extrapolated $(E_{out})_{max}$ and η_{max} for a 130 μm long sample, assuming NLC scattering and absorption losses amounting to 6.95 cm^{-1} [89].

E(μJ)	P_{NIR}(mW)	E_{out}(nJ)	η(%)	$(E_{out})_{max}$(nJ)	η_{max}(%)
0.48	0	0.01	0.003	0.04	0.010
	2	0.42	0.091	1.55	0.336
	4	1.13	0.245	4.14	0.898
	6	1.65	0.358	6.05	1.313
0.50	0	0.04	0.009	0.15	0.031
	2	0.83	0.173	3.05	0.635
	4	2.60	0.542	9.54	1.988
	6	3.85	0.803	14.14	2.945
0.55	0	0.11	0.020	0.39	0.075
	2	2.60	0.493	9.54	1.807
	4	5.77	1.093	21.16	4.007
	6	9.15	1.733	33.57	6.358
0.60	0	0.16	0.028	0.59	0.102
	2	4.73	0.822	17.36	3.014
	4	9.48	1.645	34.76	6.035
	6	15.10	2.622	55.39	9.617

Such behavior can be exploited for all-optical modulation of the random laser, i. e., the control of the RL operation by means of low-power (mW) non-resonant input beams collinear with the pump but in the extraordinary-wave polarization. Unlike previous reports where random lasing was modulated via light-induced absorption or heating [91] or via trans-cis light-induced isomerization [92], the soliton control entails the possibility of a non-dissipative NIR-driven transistor random laser, a random *trans-laser* [93,94].

Figure 5 shows the operation of such random trans-laser when switching on or off a 6 mW NIR soliton. As the soliton is formed, the RL in-out characteristic shifts to a lower pump threshold, promoting either the turn-on of the random laser or its increased efficiency, depending on the bias point represented by the pumping level. This mechanism is illustrated by extracting the peak intensity counts after either averaging over a large number (N = 200) of single-shot spectra or taking the average of the whole spectra. In either case the trans-laser can be switched-on by the presence of a collinear soliton (cases "α" in Fig. 5) or its efficiency substantially enhanced (cases "β" in Fig. 5). Below RL threshold, conversely, the nematicon changes the input-output conversion of the system in a negligible manner. Remarkably, the

Optical Materials EXPRESS

NIR-driven transition "β" in Fig. 5 corresponds to an external RL conversion efficiency increasing from 0.03% to 2.62% as the soliton is injected, with emitted laser energy going from 160 pJ to 15.1 nJ.

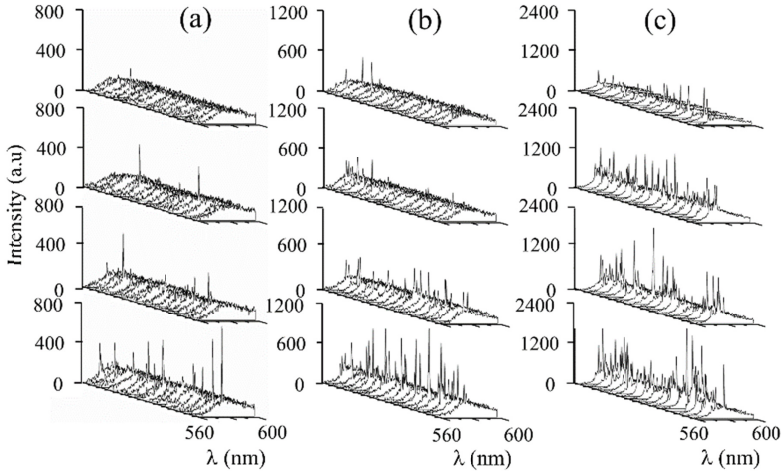

Fig. 4. Realizations of single-shot RL output intensity spectra for nematicon input powers of 0, 2, 4, 6 mW from top to bottom and pump energies (a) 0.48 μJ, (b) 0.51 μJ, (c) 0.55 μJ, respectively.

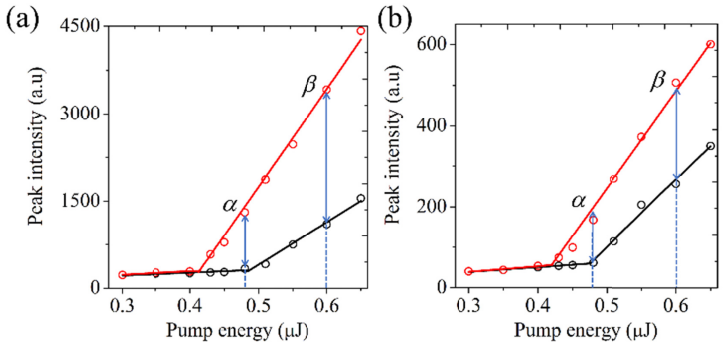

Fig. 5. (a) Peak intensity counts from averaged RL spectra (N = 200) versus pump energy/pulse without (black line and symbols) in the presence of a 6 mW nematicon (red line and symbols). (b) Same as in (a) but averaging peak intensity values from single-shot spectra (see also [94]). The transitions α and β (light blue lines and arrows) indicate possible transistor-like operations at different pump biases.

6. Beaming the emitted laser light

While the output profiles of most random lasers are typically noisy and spiky, propagating RL light within a non-resonant soliton waveguide allows each laser spike to populate guided-wave modes with real and complex eigenvalues, letting their intensity distributions overlap at the exit after propagating through the sample. When imaging the output spot of the soliton-assisted random laser, in fact, the transverse profile brought about by guided-wave confinement appears smoother and closer to a bell shape, as shown in Fig. 6(d), after propagating along the sample with the walk-off characteristic of the nematicon (Fig. 6(b). Hence, at variance with bulk RL without soliton (Fig. 6(a) and Fig. 6(c)), the RL emission acquires beam-like features with a well-defined direction and transverse distribution [93]. The angular location of the RL spot corresponds to walk-off in the NIR, close to 7° in our guest-host. At the sample exit, the RL spot is then displaced by nearly 245 μm from the position corresponding to the input wave-vectors $\boldsymbol{k}_g // \boldsymbol{k}_{NIR}$, shown by a white dashed circle in Fig. 6(d).

Optical Materials EXPRESS

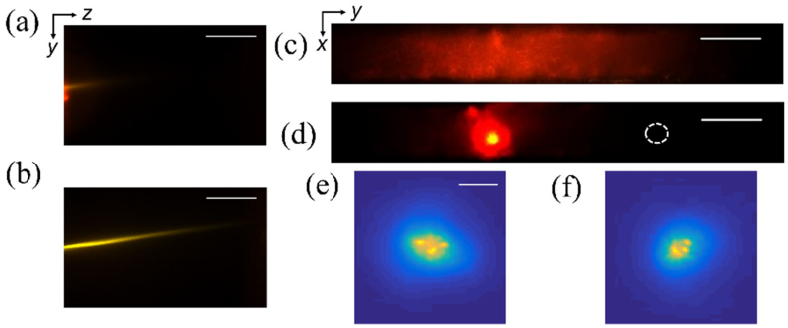

Fig. 6. (a) Photograph of emitted light in the observation plane *yz* in the absence of a NIR nematicon and for pump pulses of energy 0.55 μJ; (b) as in (a) but with a pump-collinear nematicon of 6 mW confining the emitted light. The scale bars correspond to 500 μm. (c-d) Photographs of the emitted RL light (corresponding to (a) and (b), respectively) in the transverse plane *xy* at the cell output (c) without NIR soliton or (d) in the presence of the soliton; the white dashed circle indicates the output location of an ordinary-wave propagating without walk-off along the input wave-vector. The scale bars correspond to 100 μm. (e-f) Photographs of the backward emitted RL light (above threshold) in the transverse plane *xy* at the cell entrance and in the presence of a 6 mW NIR soliton; the two realizations correspond to distinct pump pulses of energy 0.8 μJ and the scale bar to 25 μm.

The benefits of propagation in a guided-wave environment for an extended distance (2 mm) can be readily appreciated when imaging the backward emitted RL light at the entrance of the sample. Sample images of the backward emission are presented in Fig. 6(e)-(f) for two distinct pump pulses of equal energies: it can be seen that the characteristic RL spikes appear with random position and size within the spot.

7. Electro-optic steering

One of the advantages of soliton-mediated propagation is reconfigurability. The soliton waveguide, in fact, can be routed at will based on the path of the self-confined beam. In liquid crystalline soft-matter, such as NLC, this is even more within reach as the material is sensitive to external stimuli such as refractive perturbations [22,23], boundaries [24], external beams [13,16], applied voltage [12,14,15,17,18], applied magnetic field [95], etc [2,7].

Applying this routing approach to the nematicon-aided RL allows demonstrating a readdressable (cavityless) laser system in which, not only directionality is preserved despite the randomness and the lack of a resonator, but can also be adjusted by acting on the laser medium itself (rather than outside it with external means). To this extent, we prepared NLC planar cells (as described above) with transparent (Indium Tin Oxide) thin-film electrodes on the parallel glass interfaces orthogonal to *x*, in order to apply an external bias voltage with dominant electric field component along *x*. When a low-frequency electric-field perpendicular to the optic axis **n** is applied, the resulting torque on the induced NLC dipoles tends to reorient the molecules out of the plane yz of the initial anchoring, thereby rotating the principal plane which defines extraordinary-waves and so lowering the beam walk-off [12]. Eventually, when the voltage is large enough to completely reorient the optic axis along *x*, the walk-off δ vanishes and the extraordinary-wave beam launched at the input (and adiabatically readjusted to the modified principal plane in the fluid [96]) propagates with Poynting vector parallel to its own wave-vector.

Typical results of voltage-controlled steering of the RL emission in the presence of a collinear nematicon are shown in Fig. (7). As the voltage applied across the NLC thickness is increased from 0 to 2.0 V, the emitted light guided along the soliton is steered from 7° to nearly 0°. Correspondingly, as the pump energy is kept constant at 0.95 μJ/pulse -well above RL threshold-, the output spectrum changes as shown in the averaged graphs (bottom panels

Optical Materials EXPRESS

in Fig. (7)). Such spectral changes can be associated to a reduced efficiency as scattering as well as pump-NIR-emission overlap are affected by the applied bias.

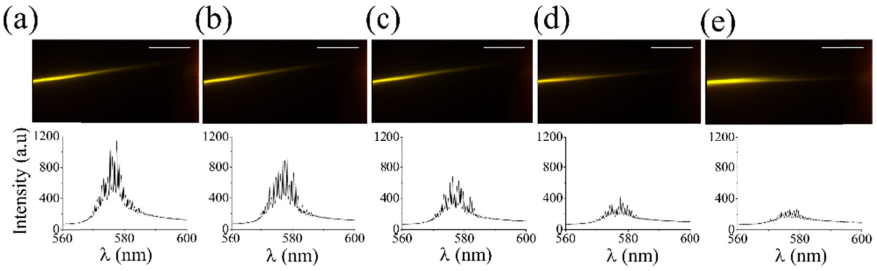

Fig. 7. (Top) Photographs and (bottom) corresponding output spectra of RL emission well above threshold (E = 0.95 μJ) upon voltage-controlled steering for (a) V = 0 V, (b) V = 0.5 V, (c) V = 1.0 V, (d) V = 1.5 V and (e) V = 2.0 V. The input NIR power for the nematicon was 5 mW.

As the beamed RL is angularly steered over nearly 7°, its output profile gets laterally displaced in the transverse coordinates, as shown for V = 0 and V = 2V in Fig. 8(a-b). A plot of measured and calculated changes in the apparent walk-off (i. e., observable walk-off in the plane *yz*) of the RL beam is presented in Fig. 8(c). It is worth stressing that, in order for the nematicon to maintain its confinement strength and guide the RL emission, complete reorientation with **n** // **x** and $\delta = 0$ cannot be reached, because in that limit the reorientational nonlinear response of the guest-host tends to zero.

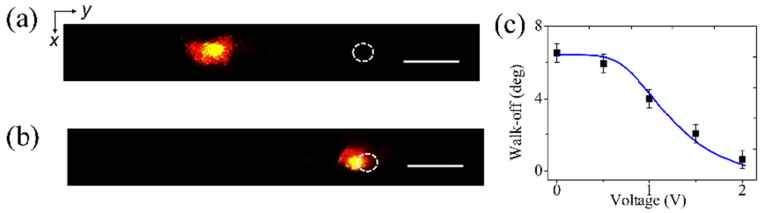

Fig. 8. (a-b) Photographs of output profiles (plane xy) of RL emission above threshold (E = 0.95 μJ) with a 5 mW nematicon and for an applied voltage of (a) V = 0 V and (b) V = 2.0 V. The white dashed circle indicates the output location corresponding to the input wave-vector; the scale bars measure a 100 μm length. (c) Calculated (solid blue line) and measured (symbols with error bars) walk-off versus applied voltage (see also [93]).

8. Magneto-optic steering

Other strategies are within reach to alter the nematicon path and steer the RL emission in this light-guided system. Since the electro-optic reorientation illustrated in the previous section causes the principal plane to rotate and, therefore, the Poynting vector to evolve versus voltage describing a cone with axis along ***k*** and half apex angle equal to δ [93]. The output RL spot, therefore, moves from $\delta = 7°$ to $\delta \approx 0°$ but - in between – it does not remain within the plane *yz*.

An alternative way to effectively steer the nematicon-assisted random laser is to apply an external magnetic field, as to magnetically reorient the NLC optic axis [95]. To this aim, we used a permanent magnet (cylindrical, 25 mm diameter) with field strength $\approx$ 0.23 T about 2 mm away from the cell output and placed on a rotating mount. Its rotation by θ_m (with respect to *z*) around *x* caused the optic axis **n** to reorient at $\theta = \theta_m$ in the *yz* plane, thereby keeping the principal plane unvaried. Then, by sweeping θ_m from −50° to 50°, the orientation θ could likewise be varied from −50° to + 50° and the walk-off δ from −7° to + 7°, while the RL

Optical Materials EXPRESS

emission spot shifted with the *yz* plane of observation, as shown for the limiting cases in Fig. 9(a-b).

Typical averaged RL spectra, obtained at pumping levels above threshold and with a 7 mW nematicon, are displayed in Fig. 9(c) together with measured and calculated walk-off of the RL-beam versus magnetic field orientation [97]. Spectra acquired for opposite angles θ_m are similar, demonstrating that the magnetic reorientation was quite efficient within the NLC volume of interest, despite the initial (boundary defined) anchoring of the optic axis **n**.

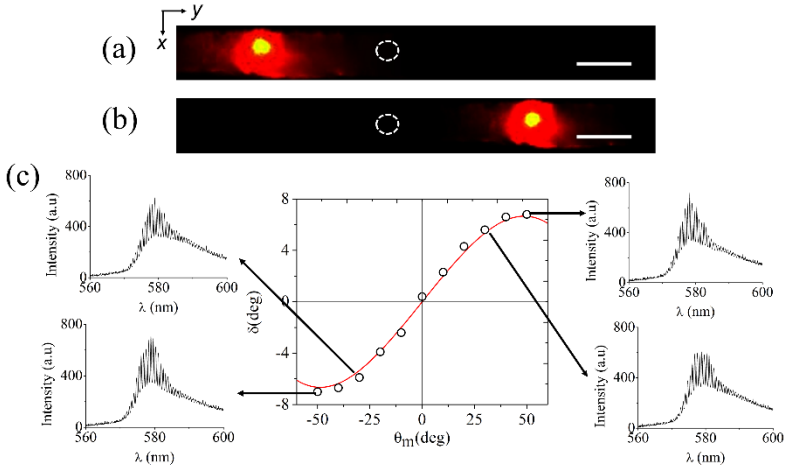

Fig. 9. (a-b) Photographs of output profiles (plane *xy*) of RL emission above threshold (E = 0.6 μJ) for a 7 mW nematicon and magnetic field along (a) $\theta_m = +50°$ and (b) $\theta_m = -50°$. The scale bars measure 100 μm. (c) Calculated (solid red line) and measured (symbols) walk-off versus θ_m, with examples of RL output spectra averaged over N = 200 pump pulses (see also [97]).

9. Conclusions and future work

The synergy of two nonlinear optical responses, namely self-focusing through reorientation and light-matter interaction for optical amplification, in conjunction with randomness and scattering has been demonstrated in a soliton-aided and soliton-controlled random laser to improve the overall performance and add novel features to this cavityless light source. Such device is able to "beam" random laser emission, improving its conversion efficiency and adding modulation capabilities in transistor-like operation driven by a small non-resonant continuous-wave input. Moreover, the emitted RL beam can be steered at will within the active medium itself, using e. g., an external voltage or magnet.

Several questions, however, remain to be answered and will require extensive future work. A model accounting for anisotropic scattering and feedback in a spatially non-homogeneous and birefringent gain medium is a formidable theoretical (and numerical) task to be undertaken. On the experimental side, the spectral features of each point within the emitted RL profile need be investigated, both in forward and in backward propagation, addressing the role of mode evolution in the graded-index light-induced channel. In terms of applications, a thorough study of time responses and their optimization when modulating the nematicon-assisted RL with electric or magnetic fields could open perspectives in sensing and speckle-free imaging.

Funding

Academy of Finland, Finland Distinguished Professor (grant no. 282858).

Acknowledgements

The authors thank R. Barboza for contributing to the experimental setup.

Optical Materials EXPRESS

References

1. D. S. Wiersma, "The physics and applications of random lasers," Nat. Phys. **4**(5), 359–367 (2008).
2. G. Assanto, *Nematicons: Spatial Optical Solitons in Nematic Liquid Crystals* (Wiley, 2012).
3. I. C. Khoo, "Nonlinear optics of liquid crystalline materials," Phys. Rep. **471**(5-6), 221–267 (2009).
4. N. V. Tabiryan, A. V. Sukhov, and B. Ya. Zel'dovich, "Orientational optical nonlinearity of liquid crystals," Mol. Cryst. Liq. Cryst. **136**(1), 1–139 (1986).
5. C. Conti, M. Peccianti, and G. Assanto, "Route to nonlocality and observation of accessible solitons," Phys. Rev. Lett. **91**(7), 073901 (2003).
6. G. Assanto and M. Karpierz, "Nematicons: self-localized beams in nematic liquid crystals," Liq. Cryst. **36**(10-11), 1161–1172 (2009).
7. M. Peccianti and G. Assanto, "Nematicons," Phys. Rep. **516**(4-5), 147–208 (2012).
8. M. Peccianti, A. Fratalocchi, and G. Assanto, "Transverse dynamics of nematicons," Opt. Express **12**(26), 6524–6529 (2004).
9. M. Peccianti and G. Assanto, "Signal readdressing by steering of spatial solitons in bulk nematic liquid crystals," Opt. Lett. **26**(21), 1690–1692 (2001).
10. M. Peccianti and G. Assanto, "Nematic Liquid Crystals: a suitable medium for self-confinement of coherent and incoherent light," Phys. Rev. E Stat. Nonlin. Soft Matter Phys. **65**(3), 035603 (2002).
11. X. Hutsebaut, C. Carbournac, M. Haelterman, J. Beeckman, and K. Neyts, "Measurement of the self-induced waveguide of a solitonlike optical beam in a nematic liquid crystal," J. Opt. Soc. Am. B **22**(7), 1424–1431 (2005).
12. M. Peccianti, C. Conti, G. Assanto, A. De Luca, and C. Umeton, "Routing of Anisotropic Spatial Solitons and Modulational Instability in liquid crystals," Nature **432**(7018), 733–737 (2004).
13. A. Pasquazi, A. Alberucci, M. Peccianti, and G. Assanto, "Signal processing by opto-optical interactions between self-localized and free propagating beams in liquid crystals," Appl. Phys. Lett. **87**(26), 261104 (2005).
14. M. Peccianti, A. Dyadyusha, M. Kaczmarek, and G. Assanto, "Tunable refraction and reflection of self-confined light beams," Nat. Phys. **2**(11), 737–742 (2006).
15. A. Piccardi, M. Peccianti, G. Assanto, A. Dyadyusha, and M. Kaczmarek, "Voltage-driven in-plane steering of nematicons," Appl. Phys. Lett. **94**(9), 091106 (2009).
16. A. Piccardi, A. Alberucci, U. Bortolozzo, S. Residori, and G. Assanto, "Readdressable interconnects with spatial soliton waveguides in liquid crystal light valves," Photon. Techn. Lett. **22**(10), 694–696 (2010).
17. J. Beeckman, K. Neyts, and M. Haeltermann, "Patterned electrode steering of nematicons," J. Opt. A, Pure Appl. Opt. **8**(2), 214–220 (2006).
18. Y. V. Izdebskaya, "Routing of spatial solitons by interaction with rod microelectrodes," Opt. Lett. **39**(6), 1681–1684 (2014).
19. M. Peccianti, C. Conti, G. Assanto, A. De Luca, and C. Umeton, "All Optical Switching and Logic Gating with Spatial Solitons in Liquid Crystals," Appl. Phys. Lett. **81**(18), 3335–3337 (2002).
20. A. Fratalocchi, A. Piccardi, M. Peccianti, and G. Assanto, "Nonlinearly controlled angular momentum of soliton clusters," Opt. Lett. **32**(11), 1447–1449 (2007).
21. M. Peccianti and G. Assanto, "Nematicons across interfaces: anomalous refraction and reflection of solitons in liquid Crystals," Opt. Express **15**(13), 8021–8028 (2007).
22. Y. Izdebskaya, A. Desyatnikov, G. Assanto, and Y. Kivshar, "Deflection of nematicons through interaction with dielectric particles," J. Opt. Soc. Am. B **30**(6), 1432–1437 (2013).
23. U. A. Laudyn, M. Kwaśny, F. A. Sala, M. A. Karpierz, N. F. Smyth, and G. Assanto, "Curved optical solitons subject to transverse acceleration in reorientational soft matter," Sci. Rep. **7**(1), 12385 (2017).
24. A. Alberucci, M. Peccianti, and G. Assanto, "Nonlinear bouncing of nonlocal spatial solitons at the boundaries," Opt. Lett. **32**(19), 2795–2797 (2007).
25. N. Karimi, M. Virkki, A. Alberucci, O. Buchnev, M. Kauranen, A. Priimagi, and G. Assanto, "Molding optical waveguides with nematicons," Adv. Opt. Mat. Commun. **5**(14), 1700199 (2017).
26. A. Piccardi, A. Alberucci, and G. Assanto, "Power-dependent nematicon steering via walk-off," J. Opt. Soc. Am. B **27**(11), 2398–2404 (2010).
27. A. Piccardi, A. Alberucci, and G. Assanto, "Self-turning self-confined light beams in guest-host media," Phys. Rev. Lett. **104**(21), 213904 (2010).
28. A. Piccardi, A. Alberucci, N. Kravets, O. Buchnev, and G. Assanto, "Power-controlled transition from standard to negative refraction in reorientational soft matter," Nat. Commun. **5**(1), 5533–5541 (2014).
29. A. Alberucci, A. Piccardi, N. Kravets, O. Buchnev, and G. Assanto, "Soliton enhancement of spontaneous symmetry breaking," Optica **2**(9), 783–789 (2015).
30. N. Kravets, A. Piccardi, A. Alberucci, O. Buchnev, M. Kaczmarek, and G. Assanto, "Bistability with Optical Beams Propagating in a reorientational medium," Phys. Rev. Lett. **113**(2), 023901 (2014).
31. A. Piccardi, N. Kravets, A. Alberucci, O. Buchnev, and G. Assanto, "Voltage driven beam bistability in a reorientational uniaxial dielectric," APL Photonics **1**(1), 011302 (2016).
32. M. Peccianti, A. Pasquazi, G. Assanto, and R. Morandotti, "Enhancement of third-harmonic generation in nonlocal spatial solitons," Opt. Lett. **35**(20), 3342–3344 (2010).
33. I. B. Burgess, M. Peccianti, G. Assanto, and R. Morandotti, "Accessible light bullets via Synergetic Nonlinearities," Phys. Rev. Lett. **102**(20), 203903 (2009).

Optical Materials EXPRESS

34. M. Warenghem, J. Blach, and J. F. Henninot, "Thermo-nematicon: an unnatural coexistence of solitons in liquid crystals?" J. Opt. Soc. Am. B **25**(11), 1882–1887 (2008).
35. U. A. Laudyn, M. Kwasny, A. Piccardi, M. A. Karpierz, R. Dabrowski, O. Chojnowska, A. Alberucci, and G. Assanto, "Nonlinear competition in nematicon propagation," Opt. Lett. **40**(22), 5235–5238 (2015).
36. U. A. Laudyn, A. Piccardi, M. Kwasny, M. A. Karpierz, and G. Assanto, "Thermo-optic soliton routing in nematic liquid crystals," Opt. Lett. **43**(10), 2296–2299 (2018).
37. V. S. Letokhov, "Generation of light by a scattering medium with negative resonance absorption," Sov. Phys. JETP **26**(4), 835 (1968).
38. P. Anderson, "Absence of diffusion in certain random lattices," Phys. Rev. **109**(5), 1492–1505 (1958).
39. A. F. Ioffe and A. R. Regel, "Non-crystalline, amorphous and liquid electronic semiconductors," Prog. Semicond. **4**, 237–291 (1960).
40. N. F. Mott, "Electrons in disordered structures," Adv. Phys. **16**(61), 49–144 (1967).
41. N. M. Lawandy, R. M. Balachandran, S. S. Gomers, and E. Sauvain, "Laser action in strongly scattering media," Nature **368**(6470), 436–438 (1994).
42. W. L. Sha, C. H. Liu, and R. R. Alfano, "Spectral and temporal measurements of laser action of Rhodamine 640 dye in strongly scattering media," Opt. Lett. **19**(23), 1922–1924 (1994).
43. H. Cao, Y. G. Zhao, H. C. Ong, S. T. Ho, J. Y. Dai, J. Y. Wu, and R. P. H. Chang, "Ultraviolet lasing in resonators formed by scattering in semiconductor polycrystalline films," Appl. Phys. Lett. **73**(25), 3656–3658 (1998).
44. H. Cao, Y. G. Zhao, S. T. Ho, E. W. Seelig, Q. H. Wang, and R. P. H. Chang, "Random Laser Action in Semiconductor Powder," Phys. Rev. Lett. **82**(11), 2278–2281 (1999).
45. V. M. Apalkov, M. E. Raikh, and B. Shapiro, "Random Resonators and Prelocalized Modes in Disordered Dielectric Films," Phys. Rev. Lett. **89**(1), 016802 (2002).
46. D. S. Wiersma and S. Cavalieri, "A temperature-tunable random laser," Nature **414**(6865), 708–709 (2001).
47. R. C. Polson and Z. V. Vardeny, "Random lasing in human tissues," Appl. Phys. Lett. **85**(7), 1289–1291 (2004).
48. G. Strangi, S. Ferjani, V. Barna, A. De Luca, C. Versace, N. Scaramuzza, and R. Bartolino, "Random lasing and weak localization of light in dye-doped nematic liquid crystals," Opt. Express **14**(17), 7737–7744 (2006).
49. C. Gouedart, D. Husson, C. Sauteret, F. Auzel, and A. Migus, "Generation of spatially incoherent short pulses in laser-pumped neodymium stoichiometric crystals and powders," J. Opt. Soc. Am. B **10**(12), 2358–2363 (1993).
50. H. Cao, Y. G. Zhao, H. C. Ong, and R. P. H. Chang, "Far-field characteristics of random lasers," Phys. Rev. B Condens. Matter Mater. Phys. **59**(23), 15107–15111 (1999).
51. S. V. Frolov, Z. V. Vardeny, K. Yoshino, A. Zakhidov, and R. H. Baughman, "Stimulated emission in high-gain organic media," Phys. Rev. B Condens. Matter Mater. Phys. **59**(8), R5284–R5287 (1999).
52. H. Cao, J. Y. Xu, D. Z. Zhang, S. Chang, S. T. Ho, E. W. Seelig, X. Liu, and R. P. H. Chang, "Spatial Confinement of Laser Light in Active Random Media," Phys. Rev. Lett. **84**(24), 5584–5587 (2000).
53. H. Cao, Y. Ling, J. Y. Xu, C. Q. Cao, and P. Kumar, "Photon Statistics of Random Lasers with Resonant Feedback," Phys. Rev. Lett. **86**(20), 4524–4527 (2001).
54. K. L. van der Molen, R. W. Tjerkstra, A. P. Mosk, and A. Lagendijk, "Spatial Extent of Random Laser Modes," Phys. Rev. Lett. **98**(14), 143901 (2007).
55. V. Milner and A. Z. Genack, "Photon Localization Laser: Low-Threshold Lasing in a Random Amplifying Layered Medium via Wave Localization," Phys. Rev. Lett. **94**(7), 073901 (2005).
56. V. M. Apalkov, M. E. Raikh, and B. Shapiro, "Random Resonators and Prelocalized Modes in Disordered Dielectric Films," Phys. Rev. Lett. **89**(1), 016802 (2002).
57. V. M. Apalkov, M. E. Raikh, and B. Shapiro, "Almost localized photon modes in continuous and discrete models of disordered media," J. Opt. Soc. Am. B **21**(1), 132–140 (2004).
58. S. Mujumdar, M. Ricci, R. Torre, and D. S. Wiersma, "Amplified Extended Modes in Random Lasers," Phys. Rev. Lett. **93**(5), 053903 (2004).
59. S. Mujumdar, V. Turck, R. Torre, and D. S. Wiersma, "Chaotic behavior of a random laser with static disorder," Phys. Rev. A **76**(3), 033807 (2007).
60. A. A. Chabanov, Z. Q. Zhang, and A. Z. Genack, "Breakdown of Diffusion in Dynamics of Extended Waves in Mesoscopic Media," Phys. Rev. Lett. **90**(20), 203903 (2003).
61. J. Fallert, R. J. B. Dietz, J. Sartor, D. Schneider, C. Klingshirn, and H. Kalt, "Co-existence of strongly and weakly localized random laser modes," Nat. Photonics **3**(5), 279–282 (2009).
62. M. Patra, "Decay rate distributions of disordered slabs and application to random lasers," Phys. Rev. E Stat. Nonlin. Soft Matter Phys. **67**(1), 016603 (2003).
63. M. Bahoura, K. J. Morris, and M. A. Noginov, "Threshold and slope efficiency of $Nd_{0.5}La_{0.5}Al_3$ $(BO_3)_4$ ceramic random laser: effect of the pumped spot size," Opt. Commun. **201**(4–6), 405–411 (2002).
64. A. Smuk, E. Lazar, L. P. Olson, and N. M. Lawandy, "Random laser action in bovine semen," Opt. Commun. **284**(5), 1257–1258 (2011).
65. A. Camposeo, P. Del Carro, L. Persano, K. Cyprych, A. Szukalski, L. Sznitko, J. Mysliwiec, and D. Pisignano, "Physically transient photonics: random *versus* distributed feedback lasing based on nanoimprinted DNA," ACS Nano **8**(10), 10893–10898 (2014).
66. A. Tulek, R. C. Polson, and Z. V. Vardeny, "Naturally occurring resonators in random lasing of -conjugated polymer film," Nat. Phys. **6**(4), 303–310 (2010).

Optical Materials EXPRESS

67. H. Cao, Y. G. Zhao, H. C. Ong, S. T. Ho, J. Y. Dai, J. Y. Wu, and R. P. H. Chang, "Ultraviolet lasing in resonators formed by scattering in semiconductor polycrystalline films," Appl. Phys. Lett. **73**(25), 3656–3658 (1998).
68. X. J. Guo, Y. F. Wang, Y. F. Jia, and W. H. Zheng, "Electrically-driven spectrally-broadened random lasing based on disordered photonic crystal structures," Appl. Phys. Lett. **111**(3), 031113 (2017).
69. A. Safdar, Y. Wang, and T. F. Krauss, "Random lasing in uniform perovskite thin films," Opt. Express **26**(2), A75–A84 (2018).
70. G. Strangi, S. Ferjani, V. Barna, A. De Luca, C. Versace, N. Scaramuzza, R. Bartolino, and R. Bartolino, "Random lasing and weak localization of light in dye-doped nematic liquid crystals," Opt. Express **14**(17), 7737–7744 (2006).
71. G. Strangi, S. Ferjani, V. Barna, A. De Luca, C. Versace, N. Scaramuzza, and R. Bartolino, "Random lasing in dye doped nematic liquid crystals: the role of confinement geometry," SPIE **6587**, 65870P (2007), doi:10.1117/12.722887.
72. S. Ferjani, V. Barna, A. De Luca, N. Scaramuzza, C. Versace, C. Umeton, R. Bartolino, and G. Strangi, "Thermal behavior of random lasing in dye doped nematic liquid crystals," Appl. Phys. Lett. **89**(12), 121109 (2006).
73. S. Ferjani, V. Barna, A. De Luca, C. Versace, and G. Strangi, "Random lasing in freely suspended dye-doped nematic liquid crystals," Opt. Lett. **33**(6), 557–559 (2008).
74. S. Ferjani, A. De Luca, V. Barna, C. Versace, and G. Strangi, "Thermo-recurrent nematic random laser," Opt. Express **17**(3), 2042–2047 (2009).
75. S. Ferjani, L. Sorriso-Valvo, A. De Luca, V. Barna, R. De Marco, and G. Strangi, "Statistical analysis of random lasing emission properties in nematic liquid crystals," Phys. Rev. E Stat. Nonlin. Soft Matter Phys. **78**(1), 011707 (2008).
76. P. G. De Gennes and J. Prost, *The Physics of Liquid Crystals* (Oxford Science, 1993).
77. G. R. Williams, S. B. Bayram, S. C. Rand, T. Hinklin, and R. M. Laine, "Laser action in strongly scattering rare-earth-metal-doped dielectric nanophosphors," Phys. Rev. A **65**(1), 013807 (2001).
78. C. J. S. de Matos, L. de S Menezes, A. M. Brito-Silva, M. A. Martinez Gámez, A. S. Gomes, and C. B. de Araújo, "Random fiber laser," Phys. Rev. Lett. **99**(15), 153903 (2007).
79. N. Lizárraga, N. P. Puente, E. I. Chaikina, T. A. Leskova, and E. R. Méndez, "Single-mode Er-doped fiber random laser with distributed Bragg grating feedback," Opt. Express **17**(2), 395–404 (2009).
80. S. K. Turitsyn, S. A. Babin, A. E. El-Taher, P. Harper, D. V. Churkin, S. I. Kablukov, J. D. Ania-Castañón, V. Karalekas, and E. V. Podivilov, "Random distributed feedback fibre laser," Nat. Photonics **4**(4), 231–235 (2010).
81. B. Abaie, E. Mobini, S. Karbasi, T. Hawkins, J. Ballato, and A. Mafi, "Random lasing in an Anderson localizing optical fiber," Light Sci. Appl. **6**(8), e17041 (2017).
82. K. C. Jorge, M. A. Alvarado, E. G. Melo, M. N. P. Carreño, M. I. Alayo, and N. U. Wetter, "Directional random laser source consisting of a HC-ARROW reservoir connected to channels for spectroscopic analysis in microfluidic devices," Appl. Opt. **55**(20), 5393–5398 (2016).
83. M. Leonetti, C. Conti, and C. Lopez, "Random laser tailored by directional stimulated emission," Phys. Rev. A **85**(4), 043841 (2012).
84. S. Schönhuber, M. Brandstetter, T. Hisch, D. Deutsch, M. Krall, H. Detz, A. M. Andrews, G. Strasser, S. Rotter, and K. Unterraniner, "Random lasers for broadband directional emission," Optica **3**(10), 1035–1038 (2016).
85. S. Bolis, T. Virgili, S. K. Rajendran, J. Beeckman, and P. Kockaert, "Nematicon-driven injection of amplified spontaneous emission into an optical fiber," Opt. Lett. **41**(10), 2245–2248 (2016).
86. S. Perumbilavil, A. Piccardi, O. Buchnev, M. Kauranen, G. Strangi, and G. Assanto, "Soliton-assisted random lasing in optically-pumped liquid crystals," Appl. Phys. Lett. **109**(16), 161105 (2016); ibid. **110**(1), 1019902 (2017).
87. N. M. Shtykov, S. P. Palto, B. A. Umanskii, D. O. Rybakov, and I. V. Simdyamkin, "Waveguide amplification of dye fluorescence in NLC layer", presented at the Workshop on Liquid Crystal Photonics (WLCP), Jastrzebia Gora (Poland) Sept. 20, 2018.
88. X. Wu, W. Fang, A. Yamilov, A. A. Chabanov, A. A. Asatryan, L. C. Botten, and H. Cao, "Random lasing in weakly scattering systems," Phys. Rev. A **74**(5), 053812 (2006).
89. S.-T. Wu and K.-C. Lim, "Absorption and scattering measurements of nematic liquid crystals," Appl. Opt. **26**(9), 1722–1727 (1987).
90. S. Perumbilavil, A. Piccardi, O. Buchnev, M. Kauranen, G. Strangi, and G. Assanto, "All-optical guided-wave random laser in nematic liquid crystals," Opt. Express **25**(5), 4672–4679 (2017).
91. H. Bian, F. Yao, H. Liu, F. Huang, Y. Pei, C. Hou, and X. Sun, "Optically controlled random lasing based on photothermal effect in dye-doped nematic liquid crystals," Liq. Cryst. **41**(10), 1436–1441 (2014).
92. C. R. Lee, S. H. Lin, C. H. Guo, S. H. Chang, T. S. Mo, and S. C. Chu, "All-optically controllable random laser based on a dye-doped polymer-dispersed liquid crystal with nano-sized droplets," Opt. Express **18**(3), 2406–2412 (2010).
93. S. Perumbilavil, A. Piccardi, R. Barboza, O. Buchnev, M. Kauranen, G. Strangi, and G. Assanto, "Beaming random lasers with soliton control," Nat. Commun. **9**(1), 3863 (2018).
94. S. Perumbilavil, M. Kauranen, and G. Assanto, "Near-infrared switching of light-guided random laser," IEEE Photonics J. **10**(5), 6100907 (2018).

Optical Materials EXPRESS

95. Y. Izdebskaya, V. Shvedov, G. Assanto, and W. Krolikowski, "Magnetic routing of light-induced waveguides," Nat. Commun. **8**, 14452 (2017).
96. A. Alberucci, M. Peccianti, G. Assanto, G. Coschignano, A. De Luca, and C. Umeton, "Self-healing generation of spatial solitons in liquid crystals," Opt. Lett. **30**(11), 1381–1383 (2005).
97. S. Perumbilavil, M. Kauranen, and G. Assanto, "Magnetic steering of directional random laser in soft matter," Appl. Phys. Lett. **113**, 121107 (2018).